

## Investigation on the Growth, Linear and Non-Linear Optical, Thermal and Photoconductivity Properties of L-Tartaric Acid-Nicotinamide Crystal

P. RAMESH KUMAR<sup>1</sup>, S. KUMARARAMAN<sup>2</sup> and P. SAGAYARAJ<sup>3,\*</sup>

<sup>1</sup>Department of Physics, Aringar Anna Government Arts and Science College, Musiri-621 211, India

<sup>2</sup>Department of Physics, Nehru Memorial College, Puthanampatti-621 007, India

<sup>3</sup>Department of Physics, Loyola College, Chennai-600 034, India

\*Corresponding author: Fax: +91 44 28175566; Tel: +91 44 28178200; E-mail: psagayaraj@hotmail.com

(Received: 5 May 2010;

Accepted: 8 November 2010)

AJC-9288

Organic materials which exhibit very large second order non-linearity with high laser damage threshold find application in the field of frequency conversion, image processing data storage, fiber optic communication *etc.*, The present work deals with the growth of L-tartaric acid-nicotinamide (LTN), an organic crystal with non-linear optical activity. The crystal has been grown by slow solvent evaporation technique and the growth conditions suitable for bulk size are optimized. The structural and morphological properties of the crystal are investigated using X-ray diffraction. The linear and non-linear optical properties of the L-tartaric acid-nicotinamide crystal are studied by FT-IR and, UV-vis-NIR spectroscopic techniques and Kurtz and Perry powder SHG test. The thermal, microhardness and photoconductivity studies are also carried out.

**Key Words:** L-Tartaric acid-nicotinamide, Non-linear optical properties, Optical band gap, Microhardness, Photoconductivity.

### INTRODUCTION

The search and design of highly efficient non-linear optical (NLO) crystals for visible and ultraviolet (UV) region are extremely important for laser processing. High quality organic NLO crystals must possess sufficient large NLO coefficient, transparency in UV region, high laser damage threshold power and easy growth with large dimension<sup>1</sup>. Organic materials attract much interest to physicists, chemists and material scientists because of their superior performance such as large NLO coefficient and ultrafast non-linear response than their inorganic counterparts.

In this connection, the study of the molecular packing and hydrogen bonding in L-tartaric acid and its derivatives is relevant to the development of approaches in crystal engineering, especially, in the field of non-linear optics<sup>2</sup>. The history of tartaric acid has long been associated with the most important discovery in the field of stereochemistry. Its industrial applications are broad and include pharmaceutical and dental materials, ceramics, paints, electrochemical coating and piezoelectronic devices<sup>3</sup>. Salts of tartaric acid with amines, amides and amino acids are long been studied for their interesting structural and, spectroscopic properties and NLO activities<sup>2</sup>. In complexes of organic bases with L-tartaric acid, one or two protons can be transferred from the carboxylic groups of tartaric acid to form the monovalent (semi-tartrate) or divalent

(tartrate) anions, respectively<sup>2</sup>. In these systems, by linking the organic molecules through hydrogen bonds, we can obtain systems with NLO and strong mechanical property. Typical representatives for such systems that have been reported in literature are; L-tartaric acid-nicotinamide, D-tartaric acid nicotinamide, urea-(d) tartaric acid (UDT), L-lysine-L-tartaric acid, L-histidinium-L-tartrate hemihydrates, 2-amino-5-nitropyridinium monohydrogen L-tartrate, *p*-nitroaniline-L-tartaric acid and 2,4,6-triamino-1,3,5-triazin-1,3-ium tartrate monohydrate<sup>1-5</sup>. Organic adduct of L-tartaric acid-nicotinamide (LTN) (2HOOCH(OH)HC(OH)COO<sup>-</sup>-2C<sub>5</sub>H<sub>4</sub>NH<sup>+</sup>CONH<sub>2</sub>·H<sub>2</sub>O) is a novel NLO crystalline material. The crystal structure of LTN is built from organic-organic complexes in which, the high optical non-linearity of organic adduct is very advantageous when compared with inorganic compounds<sup>1</sup>. The transmission range (280-1900 nm) and intense SHG signals from the LTN crystal have been reported<sup>6</sup>. Shen *et al.*<sup>1</sup> have made a systematic investigation on the growth of LTN crystal by slow cooling technique. The crystal structure was solved and the result indicated that LTN crystallizes in the monoclinic system in the space group P2<sub>1</sub>. The unit cell is composed of four L-tartaric acid, four nicotinamide and two water molecules. The simple combinations through intermolecular hydrogen bonds in the crystal are shown in Fig. 1. Hameed and Lan<sup>6</sup> studied the nucleation kinetics of LTN crystal. The SHG efficiency of LTN was found to be equal to that of KDP<sup>1</sup>.

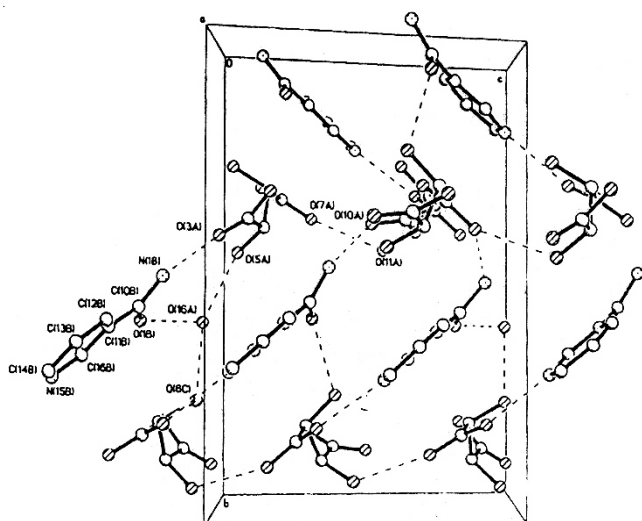


Fig. 1. Unit cell packing diagram of LTN

This article deals with our attempts to grow single crystal of L-tartaric acid-nicotinamide by slow solvent evaporation method. The physico-chemical properties of the crystal were investigated by powder XRD, UV-vis-NIR, Kurtz and Perry powder technique, FT-IR and TG/DTA. To the best of our knowledge, the optical band gap and laser damage threshold measurements, microhardness profile and photo conductivity studies are reported for the first time.

## EXPERIMENTAL

**Determination of solubility:** AR grade (Merck) L-tartaric acid (purity 99.9 %) and nicotinamide (purity 99.9 %) were bought commercially and used as purchased. In order to investigate the crystalline nature of LTN, several solvents in pure or mixture forms were investigated to grow L-tartaric acid-nicotinamide crystal. A systematic study was undertaken to determine the solubility of LTN salt in different solvents including deionized water, pure polar organic and inorganic solvents like methanol, ethanol, mixture of N,N-dimethyl formamide (DMF), DMSO and water, mixture of ethanol and water. The solubility diagram for solvents other than water is shown in Fig. 2a. Though the solubility of L-tartaric acid-nicotinamide salt is reasonably good, the solutions prepared with alcohols, DMF, DMSO and their mixtures with water have yielded very small size crystals and are predominantly in needle shape with visible inclusions. The solubility study confirmed that the deionized water is the best solvent for crystallizing good quality single crystals. The solubility diagram for L-tartaric acid nicotinamide in water at different temperatures (30, 35, 40, 45 and 50 °C) is shown in Fig. 2b. L-Tartaric acid-nicotinamide has a positive solubility coefficient in water solvent since its solubility increases with the temperature.

**Growth of L-tartaric acid-nicotinamide crystal:** L-Tartaric acid-nicotinamide was synthesized by dissolving L-tartaric acid (225 g, 1.5 mol) in deionized water that contained nicotinamide (183 g, 1.5 mol). The prepared solution was stirred magnetically for 2-3 h and then heated up to 45 °C to form saturated solution. The solution was transferred into a Petri dish and then allowed to dry. The synthesized product was further purified by repeated recrystallization (typically 3-4 times)

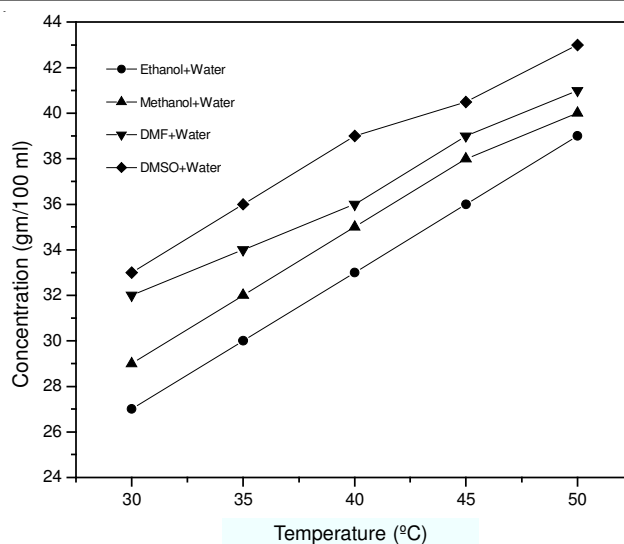


Fig. 2a. Solubility curve of LTN with different solvents

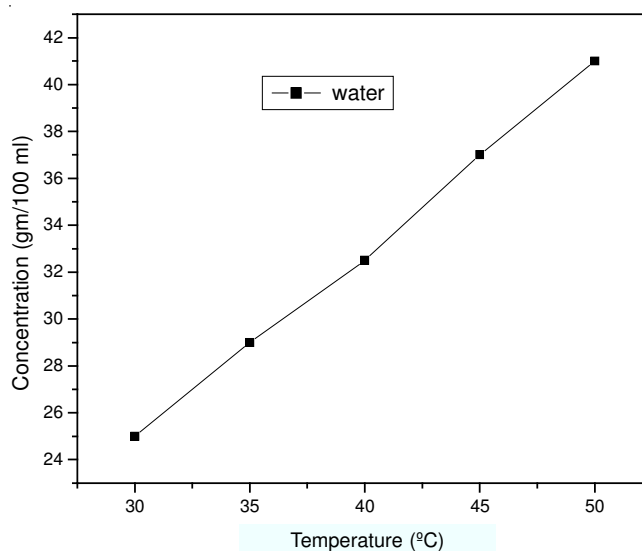


Fig. 2b. Solubility curve of LTN with water

to improve the purity. Based on the solubility data, the obtained salt of L-tartaric acid-nicotinamide was dissolved in deionized water to carry out the growth experiment. The saturated solution was prepared at 45 °C and covered with perforated lid and then it was housed in a constant temperature bath controlled with an accuracy of  $\pm 0.01$  °C. Within a week time, crystal seeds with perfect shape and high transparency were formed by spontaneous nucleation. Optically clear, defect free crystals with perfect shapes were chosen as the seeds and used for the growth experiment. The seed crystal was tied with nylon thread and then submerged into the supersaturated solution kept in the beaker. The solvent was allowed to evaporate at a constant temperature of 45 °C. After a growth period of 30 days, the crystal was harvested. The photograph of the crystal is shown in Fig. 3a. The growth morphology of LTN single crystal was studied and indexed using ENRAF NONIUS CAD4-F single crystal X-ray diffractometer and its morphology is shown in Fig. 3b. It is evident that the rate of growth is fast along the b-axis and the (0 0 1) plane is the most prominent one and the other two planes are (0 1 0) and (1 0  $\bar{2}$ ).

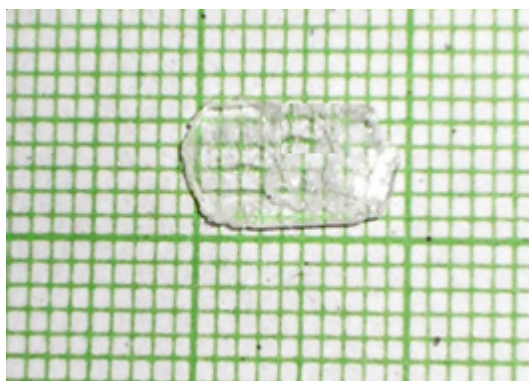


Fig. 3a. Photograph of grown LTN crystal

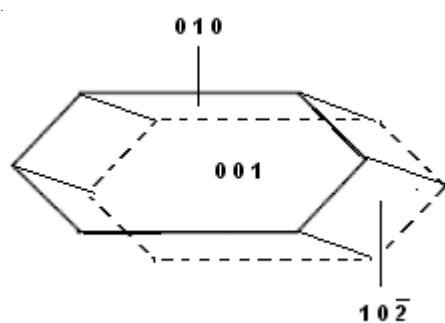


Fig. 3b. Morphology of LTN crystal

## RESULTS AND DISCUSSION

**Powder X-ray diffraction analysis:** The powder X-ray diffraction pattern of L-tartaric acid-nicotinamide crystal has been recorded on XPERT-PRO diffractometer system at a scan speed of 1.2°/min. The structure was estimated with the observed  $2\theta$  values. The PROZKI software package was employed to index the powder diffractogram (Fig. 4). The powder XRD analysis of LTN revealed its structure as monoclinic with non-centrosymmetric space group of  $P2_1$ . The calculated powder XRD data is nearly the same as those obtained from single crystal XRD analysis done by Shen *et al.*; Okaya and Stemple<sup>17</sup>. The determined lattice dimensions are;  $a = 6.237 \text{ \AA}$ ,  $b = 5.791 \text{ \AA}$ ,  $c = 7.752 \text{ \AA}$  and  $\beta = 100.21^\circ$ .

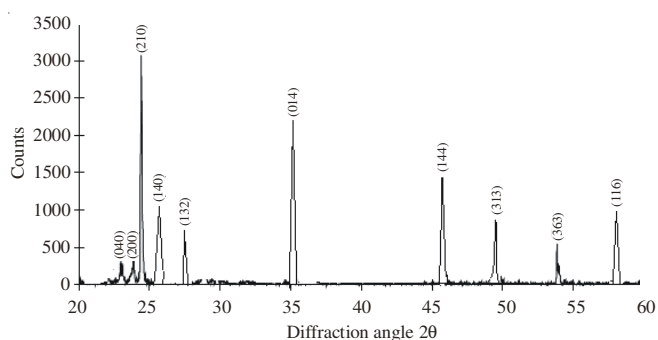


Fig. 4. Powder XRD pattern of LTN crystal

**FT-IR study:** The infrared spectrum of L-tartaric acid-nicotinamide crystal is shown in Fig. 5 and the spectral assignments are listed in Table-1. The  $\text{NH}_2$  vibrations of nicotinamide are observed at 3345 and 3148  $\text{cm}^{-1}$ . The CH vibration peak is present at 3067  $\text{cm}^{-1}$ . The C=O stretch is positioned at 1667  $\text{cm}^{-1}$ .

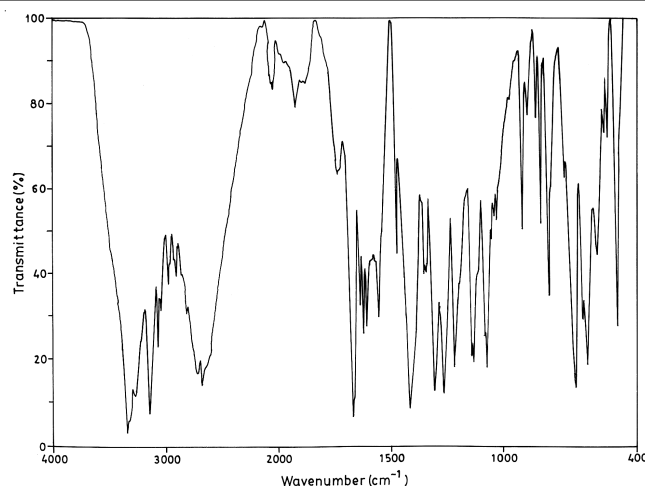


Fig. 5. FT-IR spectrum of LTN

TABLE-1  
FT-IR SPECTRAL ASSIGNMENTS OF LTN CRYSTAL

| Wavenumber ( $\text{cm}^{-1}$ ) | Assignments  |
|---------------------------------|--|
| 3309                            | $\text{NH}_2$ symmetric stretching                 |
| 3275                            | $\text{NH}_2$ asymmetric stretching                |
| 2974 and 2969                   | CH vibrations of tartaric acid                     |
| 2679 and 2717                   | Hydrogen bonded OH groupings                       |
| 1729                            | C=O stretch of tartaric acid                       |
| 1667                            | C=O stretching                                     |
| 1551 and 1414                   | $\text{COO}^-$ asymmetric and symmetric vibrations |
| 1304, 1262 and 1213             | C-O stretching and OH deformation                  |
| 1066                            | C-O stretching of alcoholic                        |

The characteristic OH vibrations of tartaric acid alcoholic group and COOH group are seen to get overlapped with the NH vibrations of nicotinamide. The characteristic CH vibrations of tartaric acid produce peaks at 2974 and 2969  $\text{cm}^{-1}$ . The intense peaks at 2679 and 2717  $\text{cm}^{-1}$  are due to hydrogen bonded OH groupings. The C=O stretch of tartaric acid gives a peak at 1729  $\text{cm}^{-1}$ . The asymmetric and symmetric COO vibrations produce peaks at 1551 and 1414  $\text{cm}^{-1}$ . The C-O stretching and OH deformation produce peaks at 1304, 1262 and 1213  $\text{cm}^{-1}$ . The alcoholic C-O stretch is seen at 1066  $\text{cm}^{-1}$ .

**UV-Vis-NIR spectral analysis:** The UV-Vis-NIR spectrum of LTN crystal was recorded in the range 200–2000 nm using VARIAN CARY 5E spectrophotometer. The recorded optical absorption spectrum of the compound is shown in Fig. 6. The absorbance is very low in the UV and the entire visible region, which is an interesting observation. The lower cut-off wavelength is found to be 250 nm. The very low value of absorbance below 900 nm is an advantage and it is a desirous property for the materials for NLO applications. Fig. 7 shows the plot of  $(\alpha h\nu)^2$  versus  $h\nu$ , where,  $\alpha$  is the optical absorption coefficient and  $h\nu$  is the energy of the incident photon. The optical energy gap ( $E_g$ ) is determined by extrapolating the straight line portion of the curve to  $(\alpha h\nu)^2 = 0$ <sup>8</sup>. The direct band gap energy ( $E_g$ ) of the LTN sample is found to be 4.6 eV.

**SHG efficiency measurement:** In order to confirm the NLO property, the grown specimen was subjected to NLO test employing Kurtz and Perry powder SHG test<sup>9</sup>. A Q-switched, mode locked Nd:YAG laser of 1064 nm and pulse width of 8 ns (spot radius of 1 mm) was used. The input laser beam

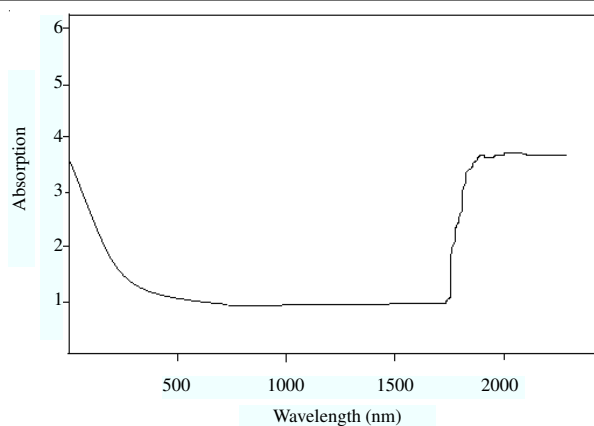


Fig. 6. UV-Vis-NIR spectrum of LTN

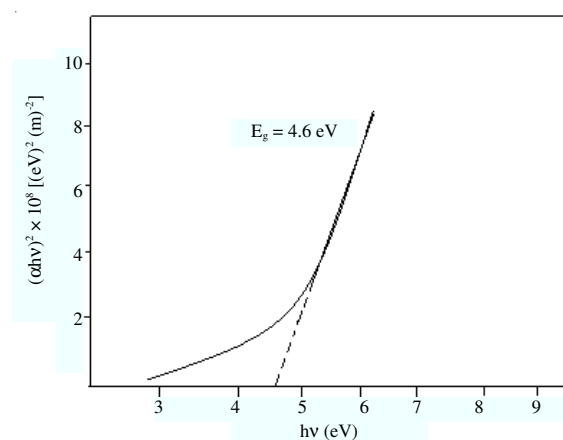


Fig. 7. Tauc's plot for LTN crystal

was directed on the sample to get maximum powder SHG. The light emitted from the sample passed through an IR filter and it was measured by means of a detector and oscilloscope assembly. The emission of green radiation from the crystal confirmed the second harmonic signal generation in the crystal. The second harmonic signal of 290 mW was obtained for LTN with reference to KDP (275 mW). Thus the SHG efficiency of LTN crystal is comparable with KDP.

**Laser damage threshold measurement:** The laser damage threshold value of the LTN crystal was measured using a Q-switched Nd:YAG laser which generates pulses at 1064 nm fundamental radiation. The grown crystal was cut and polished into a rectangular slab of area  $4 \text{ mm}^2 \times 5 \text{ mm}^2$  and then the laser damage threshold was measured. The laser beam of 1 Hz with pulse duration of 25 ps was focused by a lens on to the surface of the crystal. The damage was observed and the energy of the laser beam was measured by the power meter. The laser damage threshold value is calculated from the laser energy divided by focused area. The laser damage threshold of LTN crystal is found to be  $6.9 \text{ GW/cm}^2$  at 1064 nm. Interestingly, the laser induced surface damage threshold study of LTN crystal indicates that the material possesses much higher laser damage threshold than some of the well known organic NLO crystals like L-prolinium tartrate ( $5.9 \text{ GW/cm}^2$ ), L-arginine phosphate ( $10.0 \text{ GW/cm}^2$ ), L-alaninium maleate ( $4.9 \text{ GW/cm}^2$ ) and L-tartaric acid ( $5.4 \text{ GW/cm}^2$ )<sup>10</sup>.

**Thermal analysis:** The thermogravimetric analysis of LTN was carried out between 23 and 1200 °C in nitrogen atmosphere at a scanning rate of 10 K/min. The TGA, DTA and DTG traces of the sample are shown in Fig. 8. In the TGA trace, a minor weight loss is observed at 135.8 °C, which could be assigned to the loss of water of crystallization. The melting point of LTN was separately determined by capillary method and it was found to be 138 °C and it is close to the reported value<sup>1</sup>. Hence, it is evident that immediately after the loss of water of crystallization; the melting of the sample is completed. The TGA trace shows the origin of weight loss immediately after the loss of water of crystallization, the melting and decomposition of the sample are expected to occur in sequential manner. Hence, from this study it is concluded that the applicability of this material to NLO is limited to maximum temperature of 135 °C. In the DTA trace, there is a sharp endotherm at 138.4 °C. It is exactly matching with the melting point of LTN.

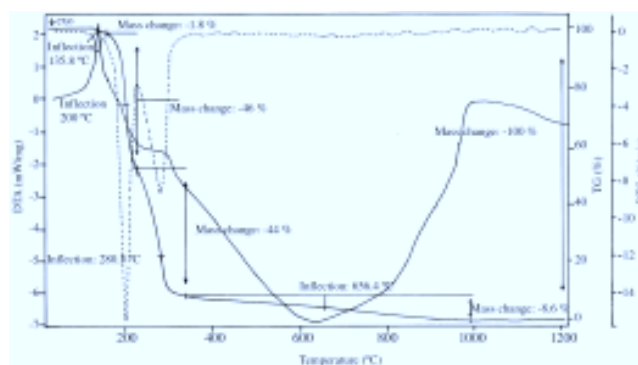


Fig. 8. TGA, DTA and DTG traces of LTN

**Microhardness study:** Mechanical strength of the materials plays a key role in device fabrication. According to Gong *et al.*<sup>11</sup> during an indentation process, the external work applied by the indenter is converted to a strain energy component which is proportional to the volume of the resultant impression. The hardness of a material is influenced by various parameters such as the lattice energy, Debye temperature, heat of formation and inter atomic spacing.

The Vickers hardness indentations were made on the cut and polished sample of LTN on the (1 0 0) plane. At room temperature, the load was varied as 10, 15, 20 and 25 g and the corresponding diagonal length of the indentation mark was measured using Vickers hardness tester (LEITZ WETZLER) fitted with Vickers diamond indenter with an incident light microscope attachment. The indentation time was kept as 5 s for all the loads. The Vickers hardness number ( $H_v$ ) was calculated using the relation,

$$H_v = 1.8544 (p/d^2) \text{ kg/mm}^2$$

where,  $p$  = applied load and  $d$  = diagonal length of the indentations. The hardness profile for LTN crystal is shown in Fig. 9a. The hardness number for a load of 10 g is  $115 \text{ kg/mm}^2$  for LTN, which is relatively a high value for the organic crystals. Usually, organic crystals suffer with reduced mechanical strength, but in the case of LTN, the calculated hardness data indicates that the grown crystal possesses improved hardness value among the solution grown organic NLO crystals and

the hardness number of the LTN crystal is much higher than conventional SHG materials like DAST ( $32 \text{ kg/mm}^2$ )<sup>12</sup> and urea ( $11 \text{ kg/mm}^2$ )<sup>13</sup>. The plot indicates that the hardness of the crystal decrease with increasing load. The decrease of the microhardness with the increasing load is in agreement with the normal indentation size effect (ISE). By plotting  $\log p$  versus  $\log d$  (Fig. 9b), the value of the work hardening coefficient 'n' of LTN has been determined as 1.59. According to Onitsch,  $1.0 \leq n \leq 1.6$  for hard materials and  $n > 1.6$  for soft materials<sup>14</sup>. Hence, it is concluded that LTN is a hard material.

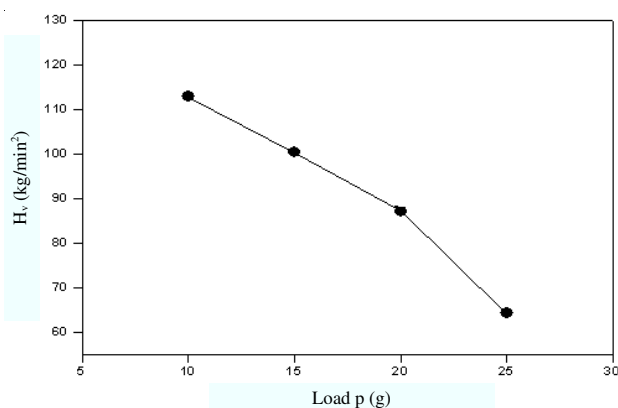


Fig. 9a. Hardness profile for LTN crystal

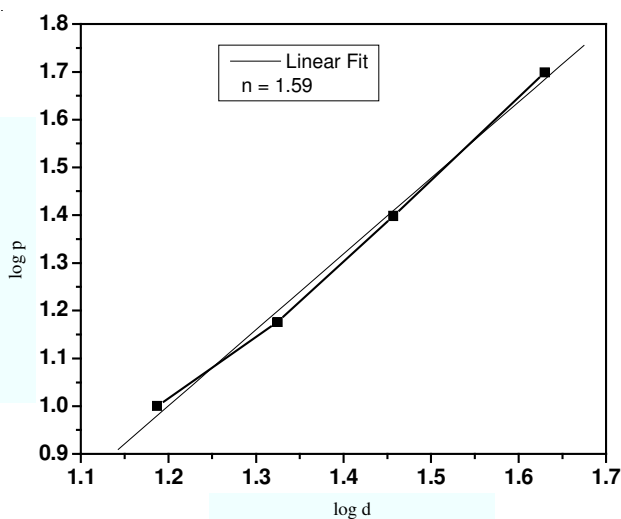


Fig. 9b.  $\log p$  versus  $\log d$  plot for LTN crystal

**Photoconductivity studies:** Polished sample of LTN crystal was attached to microscope slide and two electrodes of thin copper wire (0.14 cm diameter) were fixed by using silver paint. The sample was connected in series to a dc power supply and a picoammeter (Keithley 485). The applied voltage was increased from 0-400 V in steps of 20 V and the corresponding dark current was recorded. The sample was then exposed to the radiation from a 100 W halogen lamp containing iodine vapour and tungsten filament. The emission spectrum of the halogen lamp was observed to be a continuous one with wavelengths ranging from 300-1000 nm. The photo current ( $I_p$ ) was recorded for the same range of the applied voltage.

The field dependent dark and photo currents of LTN crystal is shown in the Fig. 10. Both the photocurrent and dark current

of LTN crystal increase linearly with applied field. It is observed from the plot that the dark current is less than that of the photo current, thus suggesting that LTN exhibits positive photoconductivity. In general positive photoconductivity is attributed to the generation of mobile charge carriers caused by the absorption of photons<sup>15</sup>.

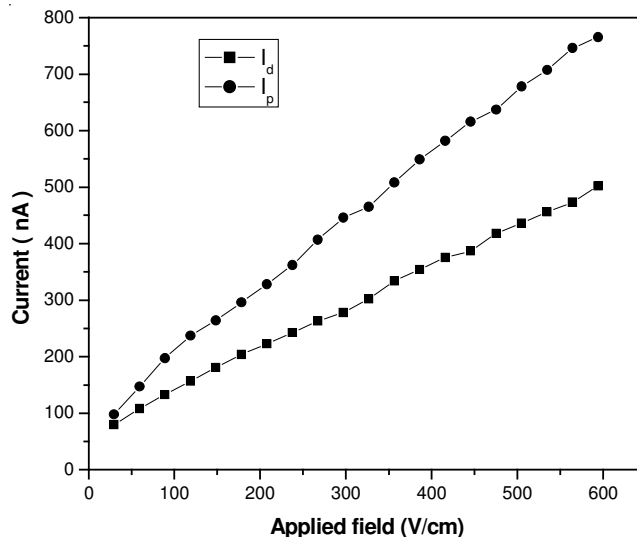


Fig. 10. Field dependent conductivity of LTN

When a semiconductor or insulator absorbs radiation of sufficient quantum energy, there is an increase of electrical conductivity called photoconductivity. Photoconductors are useful for varying electric current by means of light. Photoconductivity results if the effect of light is primarily either to increase the density of free carriers or if the effect of light is to decrease the resistance of barriers in the material. When barriers are not present, the absorption of radiation producing photoconductivity ionizes either host-crystal atoms or impurity atoms, producing free electrons and free holes or free charge carriers of just one sign, respectively. It is the change in the density of free charge carriers throughout the photoconductor which is responsible for the photoconductivity. When barriers to the flow of electrons are present, there are regions of photoconductor with a high density of free carriers separated from other similar regions by narrow regions with lower density of free carriers. The latter regions, often in the form of space-charge layers, prohibit the flow of charge carriers from one region of the photoconductor to another. The action of light in this case is to decrease the height of the barrier, thus permitting greater charge carrier flow between different regions of the photoconductor<sup>16</sup>.

## Conclusion

Single crystal of LTN was conveniently grown by slow solvent evaporation technique. Single crystal XRD studies confirm the structure of the grown crystal as monoclinic with non-centrosymmetric space group of P2<sub>1</sub>. From the FT-IR analysis, the composition and various functional groups present in the sample are identified. The optical transmission spectrum of LTN confirms the wider optical transparency from 280-1500 nm. The SHG efficiency of LTN was measured and found to be equal that of inorganic NLO crystal of KDP. The laser

damage threshold value of the sample is reasonably good. The thermal analysis of LTN confirmed the melting point of the sample as 138.4 °C and the TGA trace clearly identified the origin of major weight loss immediately after the loss of water of crystallization. The microhardness measurements indicate the hard nature of the LTN crystal. The photoconductivity study ascertains the positive photoconductivity nature of the sample. Thus the good optical as well as non-linear optical properties coupled with moderate mechanical property make L-tartaric acid-nicotinamide; a candidate material for non-linear optical and laser related applications.

#### ACKNOWLEDGEMENTS

The authors are grateful to DST-SERC for the instrumentation facility provided at Loyola College (Project SR/S2/LOP-03/2007).

#### REFERENCES

1. J. Shen, J. Zheng, Y. Che and B. Xi, *J. Cryst. Growth*, **257**, 136 (2003).
2. Z. Dega-Szafran, A. Katrusiak and M. Szafran, *J. Mol. Struct.*, **891**, 258 (2008).
3. Z. Dega-Szafran, G. Dutkiewicz, Z. Kosturkiewicz and M. Szafran, *J. Mol. Struct.*, **889**, 286 (2008).
4. P. Thorey, P. Bombicz, I.M. Szilagy, P. Molnara, G. Bansaghia, E. Szekelya, B. Simandia, L. Parkanyib, G. Pokold and J. Madarasz, *Thermochim. Acta*, **497**, 129 (2010).
5. Y. Zhang, Y. Wang, Y. Che and J. Zheng, *J. Cryst. Growth*, **299**, 120 (2007).
6. A.S. Haja Hameed and C.W. Lan, *J. Cryst. Growth*, **270**, 475 (2004).
7. Y. Okaya and N.R. Stemple, *Acta Cryst.*, **21**, 237 (1966).
8. J. Tauc's, 'Amorphous and Liquid Semiconductors', J. Tauc Ed. Plenum, New York (1974).
9. S.K. Kurtz and T.T. Perry, *J. Appl. Phys.*, **39**, 3798 (1974).
10. S.A. Martin, B. Dhas and S. Natarajan, *Cryst. Res. Tech.*, **42**, 471(2007).
11. J. Gong, G. Bhagavannarayana, R.V. Ananthamurthy, G.C. Budakoti, B. Kumar and K.S. Bartwal, *J. Appl. Cryst.*, **38**, 768 (2005).
12. S. Kalainathan and K. Jagannathan, *J. Cryst. Growth*, **310**, 2043 (2008).
13. D.P. Anand, S. Selvakumar, K. Ambujam, K. Rajarajan, M.G. Mohammed and P. Sagayaraj, *Indian J. Pure Appl. Phys.*, **43**, 463 (2005).
14. S. Mukerji and T. Kar, *Cryst. Res. Tech.*, **34**, 1323 (1999).
15. V.N. Joshi, Photoconductivity, Marcel Dekker, New York (1990).
16. R.H. Bube, Photoconductivity of Solids, Wiley Interscience, New York (1981).

### 11TH INTERNATIONAL CONFERENCE ON CARBON DIOXIDE UTILIZATION

27 — 30 JUNE, 2011

DIJON, FRANCE

*Contact:*

Pascale Bridou Buffet, FFC.

E-mail: pascale.bridou@wanadoo.fr, web site <http://www.ffc-asso.fr/ICCDU/>